Proceedings of the 17th World Congress
The International Federation of Automatic Control
Seoul, Korea, July 6-11, 2008

Robust Control Design for Resonance Damping of a Directional Microphone ⋆

Henik V. Vargas, Eva Wu, Ronald N. Miles, and Jinli Qu *

* *State University of New York at Binghamton, Binghamton, NY 13902 USA (e-mail: hvargas1,evawu,miles,jqu1@binghamton.edu).*

Abstract: This work applies μ analysis and synthesis techniques to develop a robust strategy for damping resonant modes in micromachined directional microphones of the parallel capacitive type. By properly selecting a weighting function, a robust controller is successfully designed via the D-K algorithm. Linear simulations show that the resonant mode of a directional microphone can be flattened out, and pushed to a frequency beyond the sensitivity of the human ear. The closed loop responses are free of ringing effects observed in open loop even for the worst-case parameter values.

Keywords: Microsystems, mechatronic systems, low cost MEMS

1. INTRODUCTION

This paper deals with the damping of unwanted resonance modes in directional microphones (Tan et al. [2002])and the model uncertainty that characterizes their manufacturing process. The parameter uncertainty of the microphone is addressed via standard robust synthesis techniques, and the nonlinearity of the feedback force is circumvented by placing restrictions on the magnitude of the electrostatic force. By tightly bounding the magnitude of the electrostatic force around some predetermined operating point, linearization becomes a valid approach to design and analysis.

In terms of resonance damping, this paper extends previous work presented by Wu et al. (Wu et al. [2004]) where feedback control is applied to actively damp the resonant frequency of a micromachined directional microphone of the parallel plate configuration, and the nonlinearity in electrostatic force is overcome by using a digital implementation called a sigma-delta ($\Sigma\Delta$) control-loop by the authors borrowing the sigma-delta modulator technology (Azis et al. [1996]). However, uncertainties in design model were not considered in the earlier work.

A major design limitation of a parallel plate device is the thermal noise induced by passive damping (Gabrielson [1993]), usually due to viscous flow of air between the diaphragm and the backplate that form the capacitor. Design of a low noise directional microphone requires special consideration to achieve low passive damping, such as using a porous backplate (Miles et al. [2004], Homentcovschi and Miles [2004]). Low damping however, results in severe ringing effects at the natural mode of the diaphragm, and therefore degrades the microphone performance. One possible way to avoid the adverse effects of low damping on the dynamic response is to introduce active damping into the microphone system. By introducing active damping through a control feedback loop, the microphone can be designed with low passive damping to reduce thermal noise and obtain high effective damping to improve system dynamic response (Qu et al. [2007]). A successful implementation of feedback control would also increase the bandwidth of the microphone by pushing out the resonant frequency beyond the range of human hearing.

The microphone dynamics are governed by

$$M_s = I\ddot{\theta} + c_t\dot{\theta} + k_t(\theta - \theta_o) \tag{1}$$

where I is the moment of inertia of the diaphragm, c_t and k_t are the torsional damping coefficient and the torsional stiffness respectively, θ_o is the initial angular displacement of the diaphragm, and M_s is the moment generated by the incident acoustic pressure gradient (Qu et al. [2007]). The task of designing a controller for (1) is complicated by the fact that the values for I, c_t and k_t cannot be controlled precisely during the manufacturing of the microphone. The synthesis of a controller that successfully damps the resonance of (1) in the face of the uncertainty in its parameters is the main focus of this paper. Table 1 presents experimental data showing the variation of parameters for a typical batch of micromachined directional microphones.

Table 1: Plant Parameter Data

Parameter	Nominal Value	Units	Variation
I	6.2662×10^{-15}	$Kg \cdot m^2$	10 (%)
c_t	6.5909×10^{-12}	$Kg \cdot m/s$	15 (%)
k_t	1.7331×10^{-5}	$Kg \cdot m/s^2$	10 (%)

This paper is organized as follows: Section 2 gives an overview of the directional microphone system, and establishes a suitable design model for the purpose of robust control synthesis. Section 3 formulates the control design as a μ-synthesis problem with structured uncertainty. Section 4 presents the synthesis of a robust controller

⋆ This work was supported in part by the NSF under Grant ECS -0643055, and by NIH grant 5R01DC005762-04 to RNM. The first author would also like to acknowledge the support of the State University of New York at Binghamton's Clifford D. Clark Graduate Fellowship Program for Diversity and the SUNY Alliance for Graduate Education and the Professoriate (NSF/AGEP).

that solves the μ-synthesis problem. Section 5 presents simulation results that validate the design of the robust controller.

2. DESIGN MODEL OF THE MICROPHONE

The system under consideration is a directional microphone whose principle of operation has been inspired by the auditory system of the parasitoid fly Ormia ochracea (Miles et al. [1995, 2004], Tan et al. [2002]). This fly has evolved mechanically coupled eardrums that allows it to achieve a remarkable sensitivity to sound pressure gradients despite its small size. This biologically engineered system has motivated the development of a new generation of directional microphones consisting of a hinged conductive diaphragm (about 1mm $\times$ 2mm in area, and 4 $\sim$ 5μm in thickness) that moves in response to sound pressure, and two electrically mutually isolated backplates acting as electrodes that lie side by side and are separated from the diaphragm by a small gap (about 5μm)(Miles et al. [2004], Tan et al. [2002]). The lowest resonance mode for this system depends on the actual dimensions of the device and the final layout achieved during the manufacturing process. This resonance, which is given by $\sqrt{\frac{k}{m}}$, limits the bandwidth of the system and degrades the performance of the microphone if it occurs within the frequency range of interest. It is desirable to control the system by applying an electrostatic force to damp undesirable oscillations due to resonance. This electrostatic force is nonlinear as it is proportional to the square of the voltage applied. Because of the configuration of the two isolated backplates playing the role of voltage-to-force transducers, the feedback force energizes the two backplates one at a time, through a couple of nonlinear switches. The two feedback signals pull on the corresponding side of the diaphragm to affect the damping (Wu et al. [2004]). Additionally, the capacitance between the parallel plates and the diaphragm is a function of the linear displacement x. This nonlinear force can be expressed as follows,

$$F_e = f(x)[V_o + V_s]^2 \tag{2}$$

In (2), V_o is a bias voltage, V_s is the voltage applied via feedback control, and $f(x)$ is defined as a negative function in the region of interest. Since F_e is a function of the linear displacement between the plates and the diaphragm, the governing equation in (1) can be represented in terms of force, mass, linear damping and stiffness by applying the adequate change in coordinate system $\theta = x/L$. The governing equation for the system with feedback is then expressed as

$$F_s + F_e = m\ddot{x} + c\dot{x} + kx \tag{3}$$

where F_s and F_e are the forces due to sound and electrostatic feedback respectively, and m, c, and k are the translational parameters of the system in (1). In (2), V_o can be selected to deflect the diaphragm to a desired operating point x^* satisfying

$$k(x^* - x_o) = f(x^*)V_o^2 \tag{4}$$

at the equilibrium. Due to the variability of the fabrication process of the microphone, x_o varies from device to device, and so does x^*. Let $x_s = x - x^*$. where x_s is the incremental displacements associated with the sound pressure around x^*. Subtracting (4) from (3) yields

$$m\ddot{x}_s + c\dot{x}_s + kx_s = f(x)[V_o + V_s]^2 - f(x^*)V_o^2 + F_s \tag{5}$$

By manipulating the right hand side of (5), the nonlinear terms can be rewritten in the following form:

$$V_o^2\hat{f}(\bar{x})x_s + 2V_o f(x)[1 + \frac{V_s}{2V_o}]V_s \tag{6}$$

in (6), $\bar{x}$ is between x and x^* according to the Mean Value Theorem. Now let the term $V_o^2\hat{f}(\bar{x})x_s$ be represented by an uncertain parameter k_e whose value depends on the initial displacement of the diaphragm x_o. (3) becomes,

$$m\ddot{x}_s + c\dot{x}_s + (k - k_e)x_s = 2V_o f(x)[1 + \frac{V_s}{2V_o}]V_s + F_s. \tag{7}$$

The introduction of k_e adds additional uncertainty to the stiffness parameter of the system. The term $2V_o f(x)[1 + \frac{V_s}{2V_o}]$ captures the nonlinearity in the electrostatic force applied between the plates. The nonlinearity associated with $f(x)$ is determined by the electric flux density distribution of the capacitive configuration, which can be considered linear in the device and operating range of interest. In order to minimize the effect of uncertainty due to V_s, the control voltage V_s is assumed to be sufficiently small compared to the bias voltage V_o. This assumption can be satisfied by imposing control magnitude restrictions during the design of the controller. Then, equation (6) can be approximated to the following expression:

$$m\ddot{x}_s + c\dot{x}_s + (k - k_e)x_s = k_v V_s + F_s, \tag{8}$$

where $k_v = 2V_o f(x)$. The transfer function that describes the dynamics of the system is given by

$$G_p(s) = \frac{1}{ms^2 + cs + k} \tag{9}$$

The values for k and m that define the natural frequency are uncertain parameters, where the effect of uncertain k_e has been absorbed into k. Thus the need arises to synthesize a controller that robustly stabilizes the plant despite parameter uncertainties. The damping coefficient c is also uncertain and affects the noise performance of the system. Table 1 shows the range of parameter variations.

The uncertain plan parameters can be represented in the following multiplicative form:

$$\begin{array}{c} m = \bar{m}(1 + P_m\delta_m) \\ c_d = \bar{c}(1 + P_c\delta_c) \\ k_s = \bar{k}(1 + P_k\delta_k) \end{array} \tag{10}$$

In (10), $\bar{m}, \bar{c}$ and $\bar{k}$ are nominal values; P_x reflects our knowledge about the parameter variability and δ_x normalizes that variability in the range [-1 1]. Thus, m, c_d, and k_s are the uncertain parameters of the transfer function in (9). The parameter variations assumed in this paper are $P_m = P_k = 10\%$ and $P_c = 15\%$. The presence of uncertainty in both the parameters of the nominal transfer function, as well as unknown dynamics of the system at higher frequencies, motivates the formulation of a μ-synthesis problem to introduce robustness in the response of the system. The results of this effort will be discussed in the following sections.

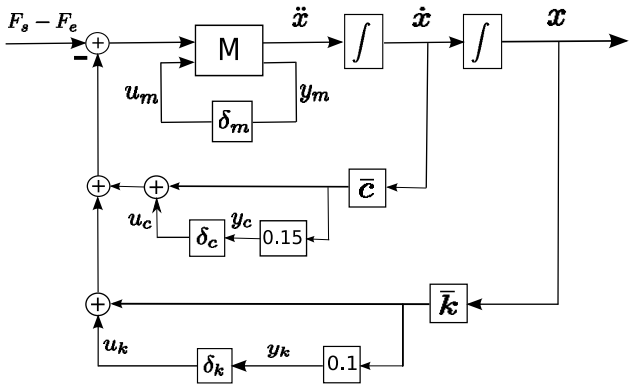

Fig. 1. Plant diagram with uncertainties isolated

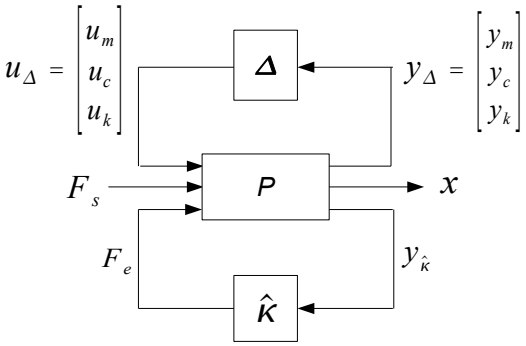

Fig. 2. General Framework for μ-Analysis/Synthesis

Many challenges still exist in the design and fabrication of the directional microphone as explained by Tan et al. [2002]. Some of those challenges include the measurement of diaphragm displacement via optical sensors and the actuation via a nonlinear electrostatic force. Nonlinearities may be assumed to be negligible by placing restrictions on the magnitude of the control signal. This allows the application of linear robust techniques to synthesize the controller. The actual performance of the system can be evaluated using nonlinear simulations.

3. μ-SYNTHESIS

In order to represent the system as a Linear Fraction Transformation (LFT) of the uncertain parameters of the plant, the uncertain parameters must be isolated (Zhou and Doyle [1998]). Figure 1 shows the interconnection of the system built from the equation of motion (1) with the uncertain parameters isolated.

The M block in figure 1 is a 2 by 2 matrix that satisfies the following LFT,

$$F_l(M, \delta_m) = \frac{1}{m}$$
$$M = \begin{pmatrix} \frac{1}{m} & \frac{-0.1}{m} \\ 1 & -0.1 \end{pmatrix} \tag{11}$$

Additionally, the δ's are isolated in separate blocks. Isolating the δ's allows the formulation of a general framework in which uncertainty is modeled as a structured block Δ as shown in equation (12).

$$\Delta = \begin{pmatrix} \delta_m & & \\ & \delta_c & \\ & & \delta_k \end{pmatrix} \tag{12}$$

Defining the Δ block allows for the uncertainty to be modeled as external inputs to the nominal plant. The overall plant, including a robust controller $\hat{\kappa}$ is shown in figure 2. The structured block Δ can be absorbed into P via an upper LFT.

$$G = F_u(P, \Delta) \tag{13}$$

Then, finding a controller that stabilizes the set of perturbed plants is reduced to minimizing the H_∞ norm of the LFT

$$\min_{\hat{\kappa}} \parallel F_l(G, \hat{\kappa}) \parallel_\infty \tag{14}$$

which can be solved via D-K iteration using the Robust Control Toolbox in Matlab, provided that an appropriate weighting function is selected to reflect performance requirements.

3.1 Performance Weighting Function W_{perf}

The design objective for this problem is the attenuation of resonant frequencies up to the maximum frequency of interest, or about 20 KHz. A successful robust design ultimately depends on the designer's ability to select an appropriate weighting function that minimizes disturbance signals (Zhou and Doyle [1998]). Therefore, a weighting function was selected to place emphasis on a frequency range which encompassed all possible resonances given the specified parameter uncertainty. The selected weighting function was found iteratively, keeping in mind that the magnitude of the sensitivity function has to be less than the inverse of W_{perf}. Hence, in order to push down the magnitude of the sensitivity function at the resonant frequencies of the entire set of uncertain plants, W_{perf} must place more weight at these frequencies. Additionally, it was found convenient to have the weighting function roll off rapidly at some point in order to keep the bandwidth of the closed loop system around 20 KHz. The resulting weighting function is a proper, rational function of third order:

$$W_{perf} = \frac{8\times10^{-5}(s+3.4\times10^6)(s+2.3\times10^5)(s+628)}{(s+1\times10^4)(s+2298)(s+1118)} \tag{15}$$

Figure 3 shows the frequency response of W_{perf}. Note that W_{perf} weighs some frequencies more than others to emphasize the design requirements, and rolls of quickly because system performance beyond a certain frequency is not important.

4. A SOLUTION TO THE μ PROBLEM

Following the selection of an appropriate weighting function, the process of finding a suitable stabilizing controller can be carried out via D-K iteration. The weighting function is placed at the output of the controller as shown in figure 4, thus W_{perf} weighs the closed loop performance, and to some degree, the magnitude of the control signal.

The feedback gain k_v is a constant proportional to $f(x)$. In order to account for nonlinearities in $f(x)$, k_v is defined as an uncertain parameter with a small variation of 0.1%.

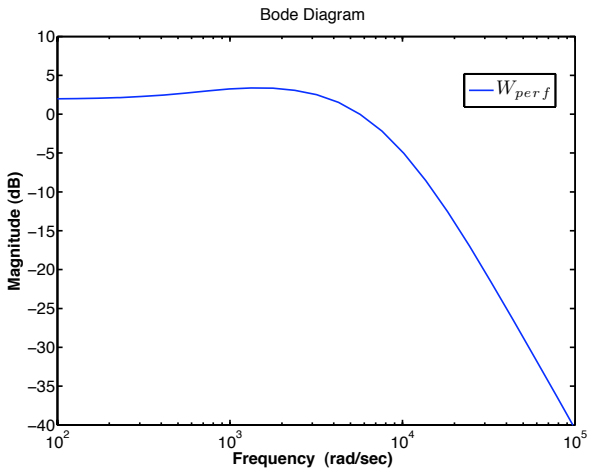

Fig. 3. Weighting Function W_{perf}

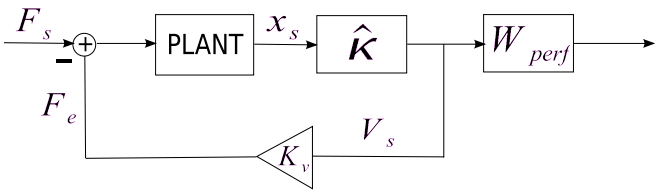

Fig. 4. Closed Loop System

This approximation is valid as long as x does not vary significantly.

μ-synthesis must be solved iteratively because the μ problem has not been fully solved (Zhou and Doyle [1998]). The D-K algorithm usually yields high order controllers that can often times be reduced to low order controllers via standard reduction techniques. In the problem being considered in this paper, approximating a high order controller by a low order one must be fairly accurate within the range of frequencies where resonance modes exist. Doing so, limits our ability to reduce a high order controller by a low order one without losing closed loop stability. Because of this, the controller being proposed here is of order 8. Table 2 lists gain, zeros, and poles of the synthesized controller.

Zeros	Poles
-1225	-1962
$-2510 \pm j52143$	-3471
$-50340 \pm j48180$	$-131 \pm j48904$
$-39475 \pm j112397$	$-36 \pm j57039$
	$-1052211 \pm j1050633$
Gain = 4913	

Table 2: Poles and Zeros of Robust Controller

Table 2 shows that the proposed controller is a strictly proper, minimum phase rational function. The effect that this controller has in the closed loop system can be investigated by comparing the open loop response (without a controller), and the closed loop response with the controller in the forward path. Figure 5 shows a comparison for both open and closed loop frequency responses, as well as the frequency response of the controller alone.

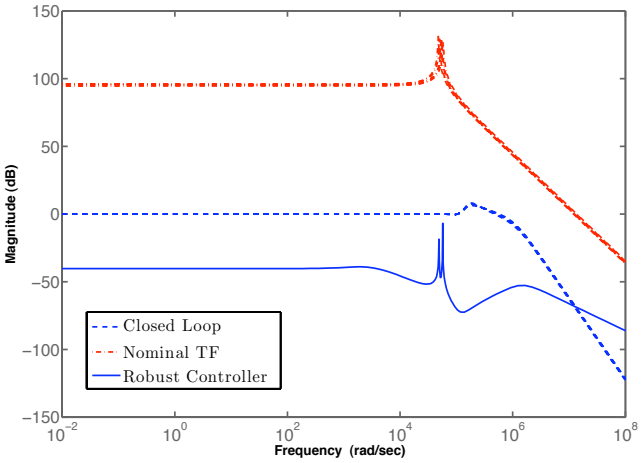

Fig. 5. Open Loop Vs. Closed Loop Responses

It should be noted that the closed loop response shown in figure 5 not only represents the dynamics of the nominal plant, but also a set of perturbed plants. In other words, figure 5 shows that the proposed controller flattens out the resonance of not only the nominal plant, but also a set of plants which reflect the variability in the parameters of (9). The bandwidth of the closed loop system is still limited by the effect of resonance, but those frequencies are now located beyond the range of sensibility of the human ear.

5. VALIDATING ROBUST PERFORMANCE

Validating the results obtained in the previous sections can be done both analytically and via simulation. In order to do robust performance analysis, another uncertain block must be defined. This performance block, Δ_f is a fictitious perturbation to the system that models performance requirements. Then, the structured perturbation block Δ can be redefined as follows:

$$\Delta_P = \begin{pmatrix} \Delta & 0 \\ 0 & \Delta_f \end{pmatrix} \tag{16}$$

The performance block Δ_f is complex valued with nominal value of 0 and norm bounded by 1:

$$\| \Delta_f \|_\infty \leq 1 \tag{17}$$

The performance perturbation block can be absorbed into the system using an upper linear fractional transformation. Now the robust performance problem becomes a regular robust stability problem with a structured perturbation block that includes a performance block (Zhou and Doyle [1998]). Using the robust control toolbox in Matlab to solve for the robust stability of the system (Balas et al. [2007]), including the perturbation in (16), shows that the closed loop system is robustly stable for the given parameter uncertainty. Furthermore, since the structured perturbation block Δ_P includes the performance block Δ_f, the closed loop system also exhibits robust performance for the modeled parameter uncertainty.

Linear simulations were performed using Simulink to verify the effect that the implementation of active damping via linear robust control techniques has on the closed loop performance of the directional microphone. The simulation

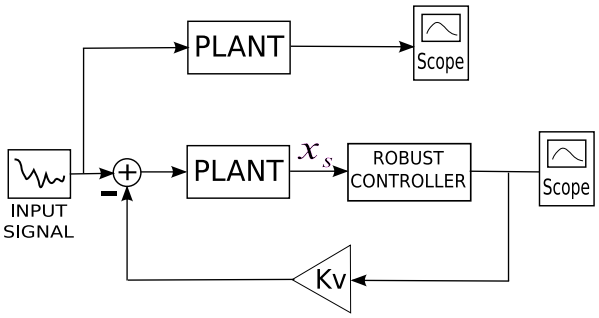

Fig. 6. Simulink Set Up for Linear Simulation

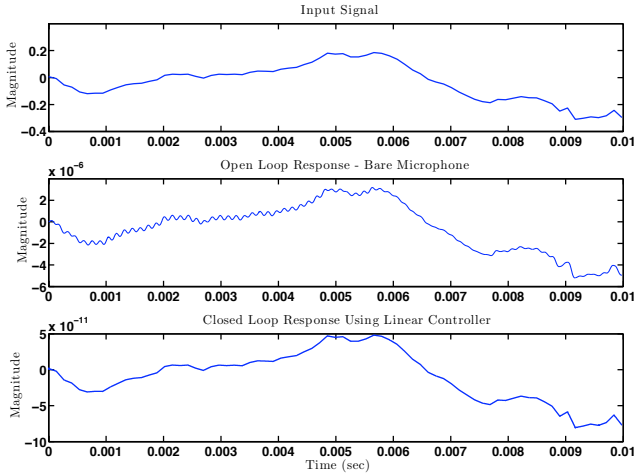

Fig. 7. Worst-Case Gain for Open Loop Vs. Closed Loop

was set up as shown in figure 6. The input data is an array with samples from a recorded sound wave. The model simulates and records data for both, open and closed loop set ups.

From a practical point of view, the real test is to find out if the proposed controller robustly stabilizes the plant when the actual parameters of the system form the so called worst-case gain (Balas et al. [2007]). That is to say, when the parameters of the uncertain plant take on values that would drive the system close to the point of instability, at least within the specified range of variability for each parameter. If it can be guaranteed that the closed loop system achieves both robust stability and performance even for the worst-case, then any other random sample taken from the family of perturbed plants must also be stable and exhibit robust performance. Figure 6 shows a comparison between the worst-case open loop response of the microphone using passive damping (No controller), and the worst-case closed loop response of the system with active damping.

It is obvious that the response of the microphone without active damping suffers considerably, thus affecting performance. This is due to the sensitivity of the system to components of the input signal that have the same frequency as the natural mode of the plant. The closed loop case however, removes the unwanted oscillations despite the fact that the parameters of the plant are the worst-case for the given variability.

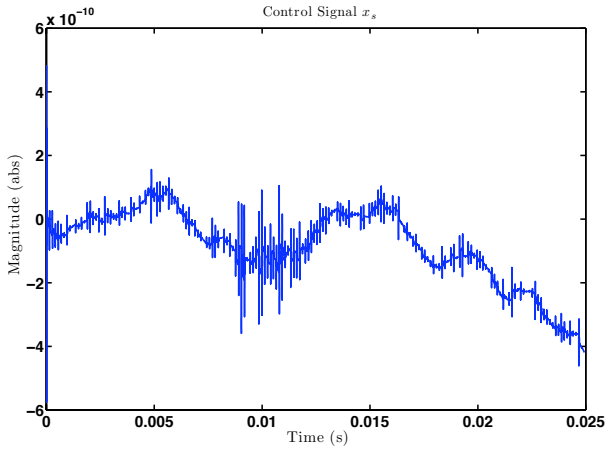

Fig. 8. Plot of x_s

Since the output of the closed loop system is the output of the controller, then the plot for the closed loop output shown in figure 7 is also the signal V_s. Therefore, the magnitude of V_s is in the order of 10^{-10}, and the value of V_o can be freely selected to satisfy assumptions made earlier to obtain (8). A suitable value of 0.1 for V_o has been proposed by Qu et al. [2007]. Furthermore, the assumption that $f(x)$ is constant can be validated by looking at the signal x_s. The assumption here is that the variation of x_s is very small, thus $f(x)$ is a constant with a small degree of uncertainty. Figure 8 shows the output of the microphone x_s. The small range of variation for x_s with respect to the separation between plates validates the assumptions made earlier for $f(x)$.

6. CONCLUSION

The main point of this paper is to prove the feasibility of applying robust control techniques to improve the performance of a MEMS device. Successful implementation of a robust controller in MEMS applications helps avoid the need to tune controllers for different samples of the same device. The strategy presented here helps alleviate the performance issues associated with parameter variability in MEMS. Consequently, a robust strategy would improve the yield during the manufacturing process and make MEMS more cost effective.

REFERENCES

P. M. Azis, H. V. Sorensen, and J. van der Spiegel. An overview of sigma-delta converters. *Signal Processing Magazine, IEEE*, 13:61–84, Jan 1996.

G. Balas, R. Chiang, A. Packard, and M. Safonov. *Getting Started with Robust Control Toolbox 3*. The Mathworks, 2007.

T. B. Gabrielson. Mechanical-thermal noise in micromachined acoustic and vibration sensors. *IEEE transactions on electron devices*, 40(5):903–909, 1993.

D. Homentcovschi and R. N. Miles. Modeling of viscous damping of perforated planar microstructures. applications in acoustics. *Acoustical Society of America Journal*, 116:2939–2947, November 2004.

R. N. Miles, D. Robert, and R. R. Hoy. Mechanically coupled ears for directional hearing in the parasitoid fly

ormia ochracea. *Acoustical Society of America Journal*, 98:3059–3070, dec 1995.

R. N. Miles, S. Sundermurthy, C. Gibbons, R. Hoy, and D. Robert. Differential microphone. United States Patent 6,788,796 B1 Sept 7, 2004.

J. Qu, N. E. Wu, R. N. Miles, and H. Vargas. Active damping of a silicon microphone using a linear controller. Submitted for publication to the American Control Conference, 2007.

L. Tan, R. N. Miles, M. G. Weinstein, R. A. Miller, Q. Su, and W. Cui. Response of a biologically inspired mems differential microphone diaphragm. *Proceedings of the SPIE AeroSense 2002*, 2002.

N. E. Wu, R. N. Miles, and O. A. Aydin. A digital feedback damping scheme for a micromachined directional microphone. *Proceeding of the 2004 American Control Conference*, 2004.

K. Zhou and J. C. Doyle. *Essentials of Robust Control*. Prentice Hall, 1998.